

Anisotropic sound and shock waves in dipolar Bose-Einstein condensate

P. Muruganandam^{a,b}, S. K. Adhikari^a

^a*Instituto de Física Teórica, UNESP - Universidade Estadual Paulista, 01.140-070 São Paulo, São Paulo, Brazil*

^b*School of Physics, Bharathidasan University, Palkalaiperur Campus, Tiruchirappalli 620024, Tamilnadu, India*

Abstract

We study the propagation of anisotropic sound and shock waves in dipolar Bose-Einstein condensate in three dimensions (3D) as well as in quasi-two (2D, disk shape) and quasi-one (1D, cigar shape) dimensions using the mean-field approach. In 3D, the propagation of sound and shock waves are distinct in directions parallel and perpendicular to dipole axis with the appearance of instability above a critical value corresponding to attraction. Similar instability appears in 1D and not in 2D. The numerical anisotropic Mach angle agrees with theoretical prediction. The numerical sound velocity in all cases agrees with that calculated from Bogoliubov theory. A movie of the anisotropic wave propagation in a dipolar condensate is made available as supplementary material.

Keywords: Dipolar Bose-Einstein condensates, sound and shock waves, Mach angle

PACS: 03.75.Kk, 67.85.-d, 47.37.+q

1. Introduction

The alkali metal atoms used in early Bose-Einstein condensate (BEC) experiments have negligible dipole moment. However, many bosonic atoms and molecules have large dipole moments and ^{52}Cr [1] and ^{164}Dy [2] BECs, with a larger long-range dipolar interaction superposed on the short-range atomic interaction, have been realized. Other atoms like ^{166}Er [3] or molecule like $^7\text{Li}-^{133}\text{Cs}$ [4] with even larger dipole moment are candidates for BEC. The superposition of short-range atomic and long-range non-local anisotropic dipolar interaction makes the study of dipolar BEC (DBEC) very challenging because of the appearance of many peculiar properties [1, 5].

A tiny object can be dragged in a BEC superfluid below the Landau critical velocity [6] without causing any change in the superfluid. Above this critical velocity, collective excitations are generated in the BEC in the form of soliton [7], turbulent vortex [7, 8] vortex-anti-vortex pair [9], and shock wave [10], etc. The critical velocity for generation of these diverse excitations have different values. It is 0.43 times the sound velocity for generation of vortices, sound velocity for the sound waves, 1.44 times the sound velocity for solitons [11]. The original Landau criterion [6] refers to the linear excitations only (phonons and rotons in He II).

One remarkable property of a DBEC is its anisotropic superfluidity [9]. In a dilute DBEC, or in a dense nondipolar BEC, like liquid helium in bulk, sound velocity could be greater than Landau critical velocity due to roton-like collective excitations [12]. The Landau critical velocity could be anisotropic in a DBEC due to anisotropic rotons [9]. Also, anisotropic soliton can be generated in a DBEC [13]. Anisotropic collapse has been observed in a ^{52}Cr DBEC

[14]. The stability of a trapped DBEC [15] also shows distinct anisotropy with a disk-shaped trap leading to more stability than a cigar-shaped one [16].

Here we consider another manifestation of anisotropic superfluidity in a DBEC, e.g., anisotropic sound and shock waves. Shock waves have been widely investigated in different systems, such as, on water surface, in supersonic jet and bullet [17] flights, in a gas bubble driven acoustically [18], in a photonic crystal [19], in the nonlinear Schrödinger equation [20] and in BEC of atoms [10], and recently observed in BEC of polaritons [7]. Using the mean-field Gross-Pitaevskii (GP) equation, we study the propagation of sound and shock waves in a uniform dilute DBEC in three dimensions (3D). Sound propagates anisotropically in a 3D DBEC of small dipole moment with larger velocity along the axial polarization direction (z) and smaller velocity in radial direction ($\rho \equiv \{x, y\}$). Consequently, sound wave emitted from a point has a non-spherical ellipsoid-like front. We study the anisotropic (oblique) waves when a tiny object is dragged along the z and x axes with shock and hypersonic velocities. The anisotropic Mach angle [17] for drag along z and x axes are in agreement with a theoretical prediction. For a critical dipole moment, the sound velocity in x - y plane falls to zero and for larger dipole moments an instability due to attraction begins.

Next we study the sound propagation in trapped DBEC, which is of interest in experiments. The effect of dipole moment is more prominent in the cigar (1D) and disk (2D) shapes with strong traps in radial and axial directions. In a spherically-symmetric 3D trap, the effect of dipole moment is less pronounced [16]. In the cigar shape, there is extra attraction due to dipole moment, and the disk shape has added repulsion. We study these 1D [21] and 2D [22]

DBEC using reduced GP equations, where the radial and axial variables are integrated out. In the disk-shaped 2D DBEC in the radial plane, dipole moment contribute to extra repulsion and this makes the system more stable. Consequently, sound propagates isotropically for all values of dipole moment with a velocity larger than that of a non-dipolar BEC. In the cigar-shaped 1D DBEC along the axial direction, dipole moment contribute to extra attraction and sound propagates with a velocity smaller than that of a non-dipolar BEC for dipole moment below a critical value. Above this critical value, instability appears due to attraction. The numerical sound velocities in 1D, 2D and 3D DBEC are in agreement with Bogoliubov theory.

2. Sound and shock waves in Dipolar BEC

We study a uniform DBEC using the GP equation [23]

$$i \frac{\partial \phi_d(\mathbf{r}, t)}{\partial t} = \left[-\frac{\nabla_d^2}{2} + \int \frac{d\mathbf{k}}{(2\pi)^d} e^{i\mathbf{k}\cdot\mathbf{r}} f_d(\mathbf{k}) \right] \phi_d(\mathbf{r}, t), \quad (1)$$

where $f_d(\mathbf{k}) = \tilde{n}_d(\mathbf{k})U_d(\mathbf{k})$, $d = 1, 2, 3$ represent 1D, 2D, and 3D, respectively, with $U_d(\mathbf{k})$ the short-range plus dipolar interaction in momentum space and $\tilde{n}_d(\mathbf{k}) \equiv \int d\mathbf{r} e^{-i\mathbf{k}\cdot\mathbf{r}} |\phi_d(\mathbf{r})|^2$ the momentum-space density. The space (\mathbf{r}) and momentum (\mathbf{k}) vectors have d components. In 3D, the interaction potential is [23]

$$U_3(\mathbf{k}) = 4\pi a + 4\pi a_{dd}\gamma(3\cos^2\theta - 1), \quad (2)$$

with $\cos\theta = k_z/k$, where θ is the polar angle. Here $\phi_d(\mathbf{r}, t)$ is the wave function at time t , a the atomic scattering length (taken to be positive here), dipole interaction strength $a_{dd} = \mu_0\mu^2 m/(12\pi\hbar^2)$, μ the (magnetic) dipole moment of an atom, and μ_0 the permeability of free space, $1 \geq \gamma \geq -1/2$ is a tuning parameter controlled by rotating orienting fields [22, 24]. In the following we use $\gamma = 1$ and shall make some comments on the consequence of negative γ on sound propagation. In Eq. (1) length is measured in units of $l_0 \equiv 1 \mu\text{m}$ and time t in units of $t_0 \equiv ml_0^2/\hbar$, where m is the mass of an atom.

The quasi-2D shape is achieved with a strong harmonic trap in the axial z direction with oscillator length $d_z = \sqrt{\hbar/m\omega_z}$, where ω_z is the angular frequency of axial trap. In this case, assuming that the axial excitations are in the oscillator ground state, the z dependence can be integrated out and in Eq. (1), we have [22]

$$U_2(\mathbf{k}) = \frac{4\pi a}{d_z\sqrt{2\pi}} + \frac{4\pi a_{dd}}{d_z\sqrt{2\pi}} h_{2D}\left(\frac{k_\rho d_z}{\sqrt{2}}\right), \quad (3)$$

with $h_{2D}(\xi) = 2 - 3\sqrt{\pi}\xi e^{\xi^2} \text{erfc}(\xi)$. The quasi-1D shape is achieved with a strong harmonic trap in radial direction with oscillator length $d_\rho = \sqrt{\hbar/m\omega_\rho}$, where ω_ρ is the angular frequency of radial trap. Then, the ρ dependence can be integrated out to obtain Eq. (1) with [21]

$$U_1(\mathbf{k}) = \frac{4\pi a}{2\pi d_\rho^2} + \frac{4\pi a_{dd}}{2\pi d_\rho^2} s_{1D}\left(\frac{k_z d_\rho}{\sqrt{2}}\right), \quad (4)$$

with $s_{1D}(\xi) = \int_0^\infty e^{-u} [3\xi^2/(u + \xi^2) - 1] du$.

2.1. Bogoliubov spectrum

The Bogoliubov spectrum of a uniform gas of density n_d is [9, 12]

$$\omega_d(\mathbf{k}) = \sqrt{(k^2/2)[k^2/2 + 2U_d(\mathbf{k})n_d]}. \quad (5)$$

In 3D, the Bogoliubov velocity of sound is [9, 12]

$$c(\theta) = \lim_{|\mathbf{k}| \rightarrow 0} \frac{\omega_3(\mathbf{k})}{|\mathbf{k}|} = c_0 \sqrt{1 + a_{dd}(3\cos^2\theta - 1)/a}, \quad (6)$$

where $c_0 = \sqrt{4\pi a n_3}$ is the sound velocity in nondipolar medium ($a_{dd} = 0$) where n_3 is density in 3D. This velocity is real for $3\cos^2\theta > 1$. For $3\cos^2\theta < 1$ ($\theta > 54.7^\circ$), the 3D velocity (6) can be imaginary for a_{dd} above a critical value, signaling an instability.

In 2D, the interaction potential (3) is always positive (repulsive) allowing sound propagation in radial direction for all a_{dd} and the Bogoliubov sound velocity is

$$c_\rho = \lim_{|\mathbf{k}| \rightarrow 0} \frac{\omega_2(\mathbf{k})}{|\mathbf{k}|} = \sqrt{2n_2\sqrt{2\pi}(a + 2a_{dd})/d_z}, \quad (7)$$

where n_2 is 2D density. If $\gamma = -1/2$ in Eq. (2), c_ρ can be imaginary corresponding to the attraction instability.

In 1D, the interaction potential (4), in the $k_z \rightarrow 0$ limit, is negative (attractive) for $a_{dd} > a$. The Bogoliubov sound velocity is

$$c_z = \lim_{|\mathbf{k}| \rightarrow 0} \frac{\omega_1(\mathbf{k})}{|\mathbf{k}|} = \sqrt{2n_1(a - a_{dd})/d_\rho^2}, \quad (8)$$

where n_1 is 1D density. The 1D sound velocity is imaginary for $a_{dd} > a$ when attraction instability appears. This instability resulting from attraction can be avoided by taking $\gamma = -1/2$.

We also calculated Gaussian variational Lagrangians [25] for the 1D and 2D GP equations [23] and found effective interactions $U_d(\mathbf{k})$, which yielded the variational sound velocities identical to the Bogoliubov results (8) and (7).

2.2. Numerical simulations

We solve the 1D, 2D, and 3D GP equations using real-time propagation with Crank-Nicolson method [26] to study sound and shock waves [10]. In 3D, we consider a generic dipolar atom for numerical simulation with $a = 4 \text{ nm}$ and background density $n_3 = 100 \mu\text{m}^{-3} \equiv 10^{14} \text{ cm}^{-3}$. To study sound propagation, a 3D Gaussian pulse is placed at the center of the uniform 3D background density given by $\phi_3^2(\mathbf{r}, 0) = [100 + 40e^{-r^2/(2w^2)}] \mu\text{m}^{-3}$, $w = 2 \mu\text{m}$ subject to the weak expulsive Gaussian potential $V(\mathbf{r}) = 0.00001e^{-r^2/(2w^2)} \mu\text{m}^{-2}$ at $t = 0$. On real-time evolution of the GP equation, the 3D Gaussian pulse expands. At large times a spherical (nondipolar BEC) or an ellipsoid-like (DBEC) sound wave front propagates outwards with a central uniform density. From the time

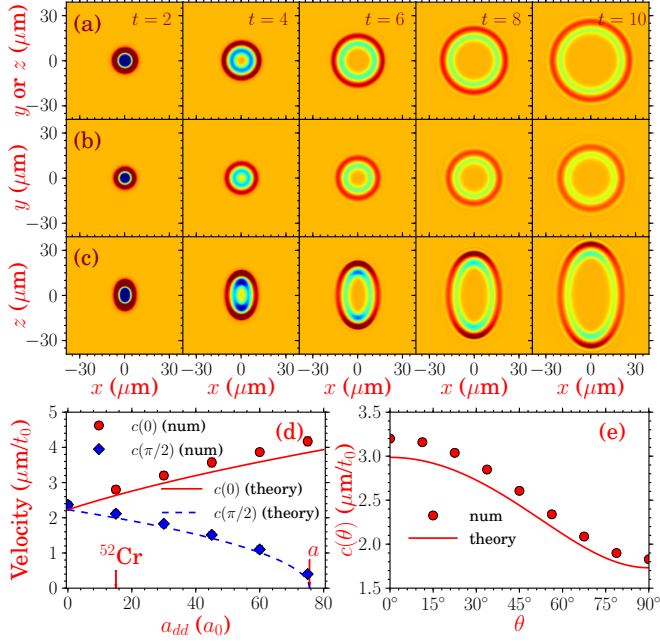


Figure 1: Contour plot of sound wave pulse (a) $|\phi_3(x, 0, z)|^2$ ($a_{dd} = 0$), (b) $|\phi_3(x, y, 0)|^2$, ($a_{dd} = 30a_0$), (c) $|\phi_3(x, 0, z)|^2$, ($a_{dd} = 30a_0$), for sound propagation from center outwards at different times $t = 2, 4, 6, 8, 10$. (d) Numerical (num) and Bogoliubov (theory) sound velocity for different a_{dd} . (e) The sound velocity $c(\theta)$ for different polar angle θ .

evolution of the sound wave front the anisotropic sound velocity in different directions is calculated.

Now we study sound propagation in 3D for a uniform DBEC. In Fig. 1 (a), we show isotropic sound propagation in x - z plane for a nondipolar BEC. In Fig. 1 (b), we show isotropic sound propagation in x - y plane [9] for a DBEC of $a_{dd} = 30a_0$. In Fig. 1 (c), we show anisotropic sound propagation in x - z plane for $a_{dd} = 30a_0$. The propagation along z direction in a DBEC has a velocity larger than that for a nondipolar BEC, whereas that in the x - y plane for a DBEC has a velocity smaller than that for a nondipolar BEC. The Bogoliubov sound velocity for nondipolar atoms is $2.242 \mu\text{m}/t_0$ compared to the numerical velocity of $2.37 \mu\text{m}/t_0$. For $a_{dd} = 30a_0$, the axial Bogoliubov sound velocity is $c(0) = 3.002 \mu\text{m}/t_0$ (numerical $3.20 \mu\text{m}/t_0$), and the radial Bogoliubov sound velocity is $c(\pi/2) = 1.741 \mu\text{m}/t_0$ (numerical $1.83 \mu\text{m}/t_0$). In Fig. 1 (d), we show the axial and radial sound velocities, $c(0)$ and $c(\pi/2)$, versus a_{dd} from numerical simulation and Bogoliubov theory with good agreement between the two. The radial velocity goes to zero for $a_{dd} = a$ and for $a_{dd} > a$ attraction instability begins. In Fig. 1 (e), we show sound velocity $c(\theta)$ versus θ for $a_{dd} = 30a_0$.

Potentials $0.2e^{-(x-v_x t)^2+z^2}/0.08 \mu\text{m}^{-2}$ or $0.2e^{-[x^2+(z-v_z t)^2]}/0.08 \mu\text{m}^{-2}$ of velocity v_x and v_z were used to study shock waves [10] in uniform 3D condensates. These potentials can be created by moving blue-detuned lasers [9]. These potentials generate waves

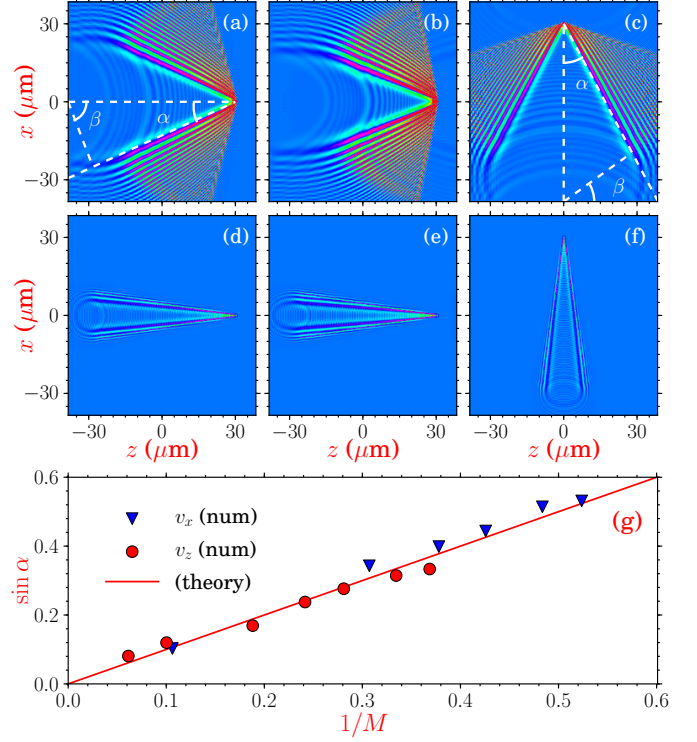


Figure 2: Contour plot of $|\phi_3(x, 0, z)|^2$ for wave propagation in a uniform 3D BEC for laser drag (a) $6 \mu\text{m}/t_0$ and (d) $30 \mu\text{m}/t_0$. The same in a DBEC with $a_{dd} = 30a_0$ for drag (b) $6 \mu\text{m}/t_0$ and (e) $30 \mu\text{m}/t_0$ along z axis and for drag (c) $6 \mu\text{m}/t_0$ and (f) $30 \mu\text{m}/t_0$ along x axis. The angles α and β are shown in (a) and (c). (g) The $\sin \alpha$ versus $1/M$ plot from theory (9) and numerical simulation (num) for different drag v_x and v_z along x and z axes in the DBEC.

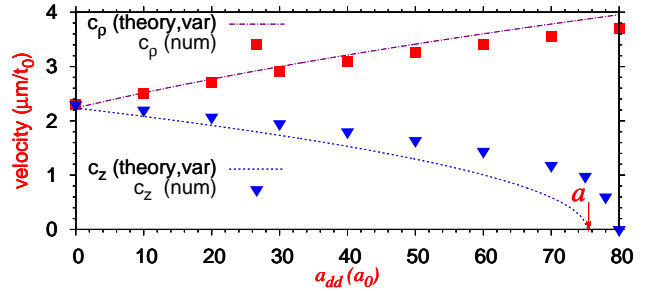


Figure 3: Numerical (num) velocity of sound propagation c_z and c_p in 1D and 2D, respectively, compared with Bogoliubov theory and variational (var) approximation.

in x - z plane along x or z direction. Typical contour plot in x - z plane of the 3D isotropic oblique wave is shown in Figs. 2 (a) and (d) for a BEC with $v_z = 6 \mu\text{m}/t_0$ (supersonic) and $30 \mu\text{m}/t_0$ (hypersonic). Anisotropic waves for a DBEC with $a_{dd} = 30a_0$ for $v_x, v_z = 6 \mu\text{m}/t_0$ and $30 \mu\text{m}/t_0$ are displayed in Figs. 2 (b), (c), (d), and (e). The Mach angle α [17] is related to laser velocity $v (= v_x, v_z)$ and polar angle β of sound propagation by

[see, Figs. 2 (a) and (c)]

$$\sin \alpha = 1/M, \quad M = v/c(\beta). \quad (9)$$

In Figs. 2 (a) and (d), $M = 6/2.37 = 2.53$, and $M = 30/2.37 = 12.66$, respectively. For a DBEC, sound velocity is different along x and z axes and α will be different for laser drag along these axes. For drag along x axis $c(\beta) = c(\alpha)$, and for drag along z axis $c(\beta) = c(\pi/2 - \alpha)$. From a full 3D simulation, for drag along x axis, in Fig. 2 (c), $\alpha \approx 31^\circ$ and $M = v_x/c(\alpha) = 6/2.99 \approx 2.01$ and for drag along z axis, in Fig. 2 (b), $\alpha \approx 18.3^\circ$ and $M = v_z/c(\pi/2 - \alpha) = 6/2.07 \approx 2.90$. At supersonic velocity, the wave with ripples outside the Mach angle is oblique, viz. Figs. 2 (a) – (c). At hypersonic velocity, the wave, mostly confined in the Mach angle, is nearly normal, viz. Figs. 2 (d) – (f). To test Eq. (9) we did simulation for different $v_x(v_z)$ and calculated α from 2D contour plots of wave propagation along x and z axes for a DBEC with $a_{dd} = 30a_0$ and obtained $c(\beta)$ and M using results in Fig. 1 (e). In Fig. 2 (g) we plot the theoretical and numerical results for $\sin \alpha$ versus $1/M$. A movie of the wave of Figs. 2 (b) and (c) is available as supplementary material [27] (also available at <http://www.youtube.com/watch?v=NR9dB7uZr9M>). Two independent simulations reported in Figs. 1 and 2 confirm the anisotropic nature of sound propagation.

Next we consider sound propagation in trapped medium. The effect of dipolar moment is more pronounced in cigar and disk shapes and we consider these two cases here. In the cigar shape, dipolar moment leads to attraction which can eventually lead to collapse for sufficiently large dipole moment. In the disk shape the system is always repulsive and propagation of sound is allowed for all values of dipole moment. The sound wave in cigar and disk shapes are studied by the reduced 1D and 2D GP equations with uniform density by putting at the center an initial Gaussian pulse on top of an expulsive Gaussian potential at $t = 0$ as in 3D. The numerical simulation was done with interactions (3) and (4) using $a = 4$ nm and $n_3 = 10^{14}$ cm $^{-3}$ and $d_z = 1$ μ m $n_2 = n_3\sqrt{2\pi}$ and $d_\rho = 1$ μ m, $n_1 = 2\pi n_3$ in 2D and 1D, respectively. This will lead to the same nondipolar sound velocity in 1D, 2D, and 3D. With time evolution, the sound wave propagates outwards from the center. In Fig. 3 sound velocities calculated for 1D and 2D propagations are plotted versus a_{dd} together with the variational and Bogoliubov sound velocities. Instability due to attraction in 1D appears for $a_{dd} > a$ from Bogoliubov theory and variational approximation. In numerical simulation the instability appears at a slightly higher value of $a_{dd} \approx 80a_0 \approx 4.23$ nm in 1D.

In this study we took the polarization along axial z axis. The conclusion about sound velocity in 1D and 2D will change if we consider the polarization along x axis. The h_{2D} of Eq. (3) will be [9] $h_{2D}(k_\rho d_z/\sqrt{2}) = -1 + 3\sqrt{\pi}k_x^2 d_z e^{\xi^2} \text{erfc}(\xi)/(\sqrt{2}k_\rho)$ yielding the 2D velocity $c_\rho = \sqrt{2n_2\sqrt{2\pi}(a - a_{dd})/d_z}$. This velocity will decrease with

increasing a_{dd} and for $a_{dd} > a$, it becomes imaginary corresponding to attraction. This instability due to attraction could be avoided by considering $\gamma = -1/2$ in Eq. (2). Also, for polarization along x axis, the 1D velocity c_z will increase with increasing a_{dd} avoiding the attraction instability.

3. Summary and Conclusion

We studied anisotropic sound and shock wave propagation in DBEC using the mean-field GP equation. In a uniform 3D DBEC, sound propagates faster along polarization (z) direction than in radial x - y plane. For $a_{dd} > a$, there is attraction instability in the radial x - y plane. Oblique waves with distinct Mach angles are formed when a tiny object is dragged with supersonic velocity in a DBEC along or perpendicular to the polarization direction. In case of a DBEC, the oblique wave is anisotropic and the modified Mach angle relation (9) is found to hold. In a quasi-2D disk-shaped DBEC, sound velocity is found to increase with a_{dd} , whereas in a quasi-1D cigar-shaped DBEC sound velocity decreases with a_{dd} and becomes zero for $a_{dd} = a$ and there is attraction instability for $a_{dd} > a$. The conditions of attraction instability can be reverted by tuning $\gamma = -1/2$ in Eq. (2). The attraction instability can be implemented by tuning the scattering length by a Feshbach resonance [16] and/or dipole moment by rotating orienting fields [24] and verified experimentally. In all cases the theoretical Bogoliubov sound velocities are in agreement with numerical simulation. Experimental confirmation is welcome for the fascinating anisotropic sound and shock wave propagation reported here.

Acknowledgements

SKA thanks Luca Salasnich for many discussions on sound waves. We thank FAPESP and CNPq (Brazil), DST and CSIR (India) for partial support.

References

References

- [1] T. Lahaye *et al.*, Nature (London) 448 (2007) 672; T. Lahaye *et al.*, Rep. Prog. Phys. 72 (2009) 126401; J. Stuhler *et al.*, Phys. Rev. Lett. 95 (2005) 150406; A. Griesmaier *et al.*, Phys. Rev. Lett. 97 (2006) 250402.
- [2] S. H. Youn, M. W. Lu, U. Ray, B. L. Lev, Phys. Rev. A 82 (2010) 043425; M. Lu, N. Q. Burdick, S. H. Youn, B. L. Lev Phys. Rev. Lett. 107 (2011) 190401.
- [3] C. I. Hancox, S. C. Doret, M. T. Hummon, L. J. Luo, J. M. Doyle, Nature 431 (2004) 281; J. J. McClelland, J. L. Hanssen, Phys. Rev. Lett. 96 (2006) 143005.
- [4] J. Deiglmayr *et al.*, Phys. Rev. Lett. 101 (2008) 133004.
- [5] D. H. J. O'Dell, S. Giovanazzi, C. Eberlein, Phys. Rev. Lett. 92 (2004) 250401; D. C. E. Bortolotti, S. Ronen, J. L. Bohn, D. Blume, Phys. Rev. Lett. 97 (2006) 160402;

- M. Asad-uz-Zaman, D. Blume, Phys. Rev. A 83 (2011) 033616;
M. Abad, M. Guilleumas, R. Mayol, M. Pi, D. M. Jezek, Phys. Rev. A 79 (2009) 063622;
P. Muruganandam, R. Kishor Kumar, S. K. Adhikari, J. Phys. B 43 (2010) 205305;
P. Muruganandam, S. K. Adhikari, J. Phys. B 44 (2011) 121001;
L. E. Young-S, P. Muruganandam, S. K. Adhikari, J. Phys. B 44 (2011) 101001.
- [6] L. D. Landau, E. M. Lifshitz, *Fluid Mechanics*, (Pergamon Press, London, 1987).
- [7] A. Amo *et al.*, Science 332 (2011) 1167.
- [8] E. A. L. Henn *et al.*, Phys. Rev. Lett. 103 (2009) 045301.
- [9] C. Ticknor, R. M. Wilson, J. L. Bohn, Phys. Rev. Lett. 106 (2011) 065301;
R. M. Wilson, S. Ronen, J. L. Bohn, Phys. Rev. Lett. 104 (2010) 094501.
- [10] B. Damski, Phys. Rev. A 69 (2004) 043610;
I. Kulikov, M. Zak, Phys. Rev. A 67 (2003) 063605;
A. M. Kamchatnov, A. Gammal, R. A. Kraenkel, Phys. Rev. A 69 (2004) 063605;
L. Salasnich *et al.*, Phys. Rev. A 75 (2007) 043616;
I. Carusotto, S. X. Hu, L. A. Collins, A. Smerzi, Phys. Rev. Lett. 97 (2006) 260403;
Yu. G. Gladush, G. A. El, A. Gammal, A. M. Kamchatnov, Phys. Rev. A 75 (2007) 033619;
L. Salasnich, Europhys. Lett. 96 (2011) 40007;
Yu. G. Gladush *et al.*, Phys. Rev. A 79 (2009) 033623.
- [11] T. Frisch, Y. Pomeau, S. Rica, Phys. Rev. Lett. 69 (1992) 1644;
T. Winiecki, J. F. McCann, C. S. Adams, Phys. Rev. Lett. 82 (1999) 5186.
- [12] L. Santos, G. V. Shlyapnikov, M. Lewenstein, Phys. Rev. Lett. 90 (2003) 250403;
R. M. Wilson, S. Ronen, J. L. Bohn, H. Pu, Phys. Rev. Lett. 100 (2008) 245302.
- [13] I. Tikhonenkov, B. A. Malomed, A. Vardi, Phys. Rev. Lett. 100 (2008) 090406;
R. Nath, P. Pedri, L. Santos, Phys. Rev. Lett. 102 (2009) 050401.
- [14] T. Lahaye *et al.*, Phys. Rev. Lett. 101 (2008) 080401.
- [15] A. Görlitz *et al.*, Phys. Rev. Lett. 87 (2001) 130402.
- [16] T. Koch *et al.*, Nature Phys. 4 (2008) 218 (2008).
- [17] E. Mach, and P. Salcher, Sitzungsberichte (Viena) 95 (1887) 764.
- [18] M. P. Brenner, S. Hilgenfeldt, D. Lohse, Rev. Mod. Phys. 74 (2002) 425.
- [19] E. J. Reed, M. Soljačić, J. D. Joannopoulos, Phys. Rev. Lett. 90 (2003) 203904.
- [20] A. M. Kamchatnov, R. A. Kraenkel, B. A. Umarov, Phys. Rev. E 66 (2002) 036609.
- [21] S. Sinha, L. Santos, Phys. Rev. Lett. 99 (2007) 140406;
F. Deuretzbacher, J. C. Cremon, S. M. Reimann, Phys. Rev. A 81 (2010) 063616.
- [22] P. Pedri, L. Santos, Phys. Rev. Lett. 95 (2005) 200404;
U. R. Fischer, Phys. Rev. A 73 (2006) 031602.
- [23] K. Góral, L. Santos, Phys. Rev. A 66 (2002) 023613;
S. Yi, L. You, Phys. Rev. A 63 (2001) 053607.
- [24] S. Giovanazzi, A. Görlitz, T. Pfau, Phys. Rev. Lett. 89 (2002) 130401.
- [25] P. Muruganandam, S. K. Adhikari, Laser Phys. (in press);
arXiv:1111.2272.
- [26] P. Muruganandam, S. K. Adhikari, Comput. Phys. Commun. 180 (2009) 1888;
P. Muruganandam, S. K. Adhikari, J. Phys. B 36 (2003) 2501;
S. K. Adhikari, P. Muruganandam, J. Phys. B 35 (2002) 2831.
- [27] See supplemental material at for a movie of anisotropic DBEC wave propagation in x - z plane. of a DBEC with $a_{dd} = 30a_0$.